A High-Level *Ab Initio* Study of the $N_2 + N_2$ Reaction Channel

Leonardo Pacifici,*[a] Marco Verdicchio,[b] Noelia Faginas Lago,[a] Andrea Lombardi,[a] and Alessandro Costantini[c]

A new six-dimensional (6D) global potential energy surface (PES) is proposed for the full range description of the interaction of the $N_2(^1\Sigma_g^+)+N_2(^1\Sigma_g^+)$ system governing collisional processes, including N atom exchange. The related potential energy values were determined using high-level *ab initio* methods. The calculations were performed at a coupled-cluster with single and double and perturbative triple excitations level of theory in order to have a first full range picture of the PES. Subsequently, in order to accurately describe the stretching of the bonds of the two interacting N_2 molecules by releasing the constraints of being considered as rigid rotors, for the same molecular geometries higher level of theory multi reference calculations were performed. Out of the calculated values a 6D 4-atoms global PES was produced for use in dynamical calculations. The *ab initio* calculations were made possible by the combined use of High Throughput Computing and High Performance Computing techniques within the frame of a computing grid empowered molecular simulator. © 2013 Wiley Periodicals, Inc.

DOI: 10.1002/jcc.23415

Introduction

Weakly bound molecular clusters and complexes are very important in gas phase chemistry both at high temperature, like that of spacecraft reentry in the atmosphere,[1,2] and at low temperature, like that of astrochemistry processes.[3] This is the case for the H_2-H_2 and N_2-N_2 systems for which in the last three decades a certain number of theoretical and experimental investigations have been carried out.[4–7] For example, a reliable and versatile potential energy surface (PES) developed for the $(H_2)_2$ system[8] was used by some of us for extended dynamical calculations.[9–13]

Quite recently, we have turned our attention into the building of a suitable PES for investigating the dynamics of the N_2-N_2 system[14] for which how to describe the long range interaction including the N_2 stretching for the nonreactive channels is still being debated.[15] A first attempt to model a reliable and versatile PES for N_2-N_2 was, in fact, performed some time ago by fitting a Lennard-Jones potential to the second virial coefficient and solid state data.[16–18] More recently, *ab initio* (for short range) and experimental (for long range) data were combined together in order to improve the formulation of the $(N_2)_2$ PES[19,20] by van der Avoird, Wormer, and Jansen,[21] without being able, however, to reproduce most of the available experimental and theoretical information.[22,23] The first $(N_2)_2$ fully *ab initio* PES was built by Stallcop and Partridge[24] by matching short and intermediate range potential energy data calculated at the coupled-cluster with single and double and perturbative triple excitations (CCSD(T)) level of theory, with those obtained for the Van der Waals region from the evaluation of the second virial coefficients. Very recently, Hellmann[25] has built an *ab initio* four-dimensional PES for N_2-N_2 in which the two interacting nitrogen molecules are considered as rigid bodies. The calculations were performed for 408 molecular geometries and 26 angular configurations at the CCSD(T) level of theory and using basis sets of the type aug-cc-pV5Z. Therefore, the complete determination of the interaction energy of the $(N_2)_2$ dimer and the construction of an accurate full dimensional PES including N atom exchange is still far from being achieved. This is also due to the lack of experimental measurements of the nitrogen dimer reactivity due to its optical inactivity. For this reason, we started a long term project within the frame of a recently established procedure for carrying out virtual experiments[26,27] and we embarked ourselves in the high level *ab initio* determination of the $N_2 + N_2$ interaction by making use of a grid enabled *ab initio* molecular simulator called grid empowered molecular simulator (GEMS).[28–30] GEMS is articulated in three blocks, INTERACTION, DYNAMICS, and OBSERVABLES, of a workflow which enables the coordinated execution of in-house developed and commercial codes on the distributed platform of European Grid Infrastructure (EGI),[31] by properly selecting among available High Performance Computing (HPC) and High Throughput Computing (HTC) grid resources. As a matter of fact, in our work within the COMPCHEM[32] Virtual Organization (VO) of the

[a] *L. Pacifici, N. F. Lago, A. Lombardi*
Department of Chemistry, University of Perugia, via Elce di Sotto, 8, Perugia, 06123, Italy
E-mail: xleopac@gmail.com
[b] *M. Verdicchio*
CNRS-Laboratoire Reactions Et Genie Des Procedes (LRGP), ENSIC, Nancy, France
[c] *A. Costantini*
INFN Perugia Section, via A. Pascoli 06123 Perugia
Contract grant sponsor: The EGI-Inspire project; Contract grant number: 261323; Contract grant sponsor: The MIUR PRIN 2008; Contract grant number: 2008KJX4SN 003; Contract grant sponsor: The MIUR PRIN 2010-2011; Contract grant number: 2010ERFKXL_002; Contract grant sponsor: The ESA-ESTEC; Contract grant number: 21790/08/NL/HE; Contract grant sponsor: The Phys4Entry (Planetary Entry Integrated Models) FP7/2007-2013 project; Contract grant number: 242311

Chemistry and Molecular & Materials Sciences and Technologies Community, we started a systematic electronic structure investigation by performing MP2 (second-order Møller–Plesset perturbation theory)[33] *ab initio* calculations[14] for a large number of nuclear geometries of the $N_2(^1\Sigma_g^+)+N_2(^1\Sigma_g^+)$ system including the nitrogen atom exchange process channel. For that purpose, a relatively small basis set of the cc-pVTZ (correlation consistent polarized valence triple-zeta) type involving 140 Gaussian functions and a correction of the basis set superposition error (BSSE) via the full counterpoise procedure[34] was adopted.

In the present article, we discuss our recent development of the calculations carried out for the same geometries using CCSD(T) and higher level methods according to the following scheme: in System Coordinates Section, the coordinate system used and the arrangements investigated are presented; in CCSD(T) Calculations Section, the results of coupled-cluster calculations, with N_2 at equilibrium distance, are illustrated; in CCSD(T) Fit Section, the fit of the CCSD(T) values to build up a first PES is discussed. Then, in Higher Level Calculations and MRPT2 PES Section, the results of higher level Multi Reference (MR) *ab initio* calculations are analyzed and matched with the CCSD(T) ones in order to produce an improved full dimensional PES. Conclusions are reported in Conclusions Section.

System Coordinates

In order to begin the calculation of the electronic structure of a molecular system one has to choose the coordinates to use for defining its geometry. According to the fact that we have included in our study geometries with the two nitrogen molecules far from equilibrium, we had to take into account both intermolecular and intramolecular degrees of freedom, together with the angular variables. For this reason, we made use of the following six variables (three angular and three radial, see Fig. 1): the angles θ_a and θ_b defining the orientation of the two diatomic internuclear vectors $\mathbf{r}_a$ and $\mathbf{r}_b$ with respect to the *z* axis of the space fixed frame, that coincides with the line passing through the centers of mass of the two N_2 molecules *a* and *b*; the dihedral angle Φ formed by the plane defined by diatom *a* and the *z* axis and the plane formed by diatom *b* and the same axis; the distance *R* between the centers of mass of the two N_2 molecules; the two intramolecular distances r_a and r_b moduli of the $\mathbf{r}_a$ and $\mathbf{r}_b$ vectors. Most of the arrangements of the N_2-N_2 system considered for the calculations are defined by one of the five different θ_a, θ_b, Φ triples illustrated in Figure 2 and generated by varying *R* from 1 to approximately 10 Å at r_a and r_b fixed at their equilibrium value ($r_a = r_b = 1.094$ Å[35]). This led to arrangements belonging to different symmetry groups: D_{2h} (90, 90, 0; *R*), D_{2d} (90, 90, 90; *R*), $D_{\infty h}$ (0, 0, 0; *R*), C_{2v} (0, 90, 0; *R*), C_{2h}(45, 45, 0; *R*), labeled in Figure 2 as H (parallel), X (X-shaped), I (linear), T (T-shaped), and Z (Z-shaped), respectively. A certain number of geometries were generated to end of mimicking the effect of stretching the nitrogen bonds by assigning to r_a and r_b the following nonequilibrium values: $r_a = 1.094$ Å and $r_b = 1.694$ Å; $r_a = 1.494$ Å and $r_b = 1.694$ Å; $r_a = 1.694$ Å and $r_b = 1.694$ Å; $r_a = 1.094$ Å and $r_b = 0.994$ Å; $r_a = 0.994$ Å and $r_b = 0.994$ Å. Some calculations were also performed using the just mentioned internuclear distance pair values and distorting gradually the H parallel arrangement into the X crossed one. For this purpose, the Φ angle was varied from 0° (H shape) to 90° (X shape) in steps of 15° in order to better characterize the possible gradual change of arrangement (P15, P30, P45, P60, P75). A summary of the structural parameters of the investigated arrangements is given in Table 1.

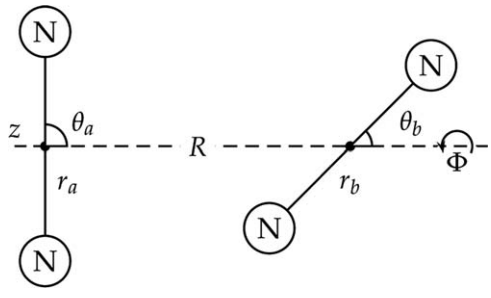

Figure 1. Scheme of the radial and angular variables adopted to define the geometry of the $(N_2)_2$ system.

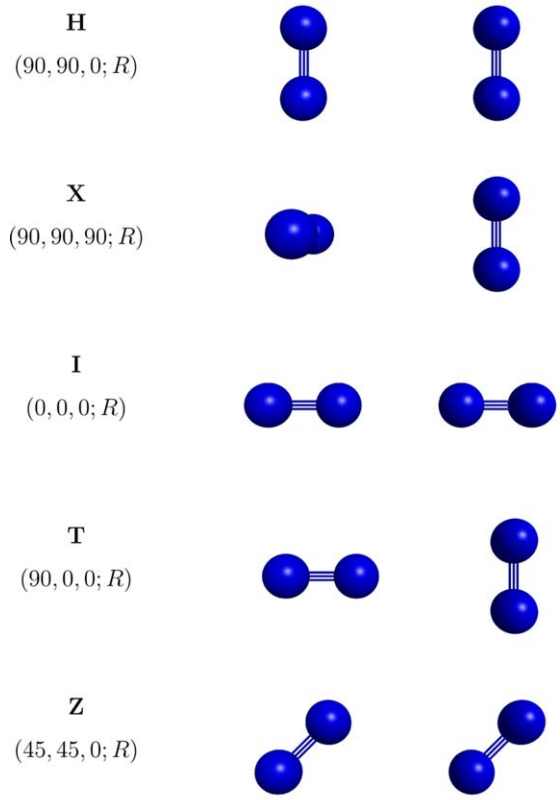

Figure 2. Sketch of the main five arrangements. [Color figure can be viewed in the online issue, which is available at wileyonlinelibrary.com.]

CCSD(T) Calculations

The adoption of the CCSD(T) level of theory for the calculation of the $(N_2)_2$ intermolecular interaction was prompted by the analysis of the large BSSE, that unphysically lowers the energy

Table 1. Summary of the structural parameters of the investigated arrangements.

	Φ(degree)	θ_a (degree)	θ_b (degree)	r_a (Å)	r_a (Å)
H	0	90	90	1.094	1.094
	0	90	90	1.094	1.694
	0	90	90	1.494	1.694
	0	90	90	1.694	1.694
P15…P75	15…75	90	90	1.094	1.094
	15…75	90	90	1.094	1.694
	15…75	90	90	1.494	1.694
	15…75	90	90	1.694	1.694
X	90	90	90	1.094	1.094
	90	90	90	1.094	1.694
	90	90	90	1.494	1.694
	90	90	90	1.694	1.694
I	0	0	0	1.094	1.094
T	0	90	0	1.094	1.094
Z	0	45	45	1.094	1.094

in the short range region, of the previously computed MP2/cc-pVTZ values.[14] CCSD(T) calculations were performed using the GAMESS-US package[36,37] and a cc-pV5Z[38,39] basis set made of a total of 420 Gaussian contractions (which eliminated the need for a BSSE correction) for the H, X, I, T, Z, P15, P30, P45, P60, and P75 arrangements. The large size of the matrices implied by such choice prompts very large memory requests and very long computing time, three orders of magnitude higher than for the cc-pVTZ basis set. For comparison, the computational costs of four different basis sets, varying from the smaller cc-pVDZ to the larger cc-pV5Z, measured on a popular processor are shown in Table 2. As may be seen from the table, the cc-pV5Z calculations make use of memories of 5.4 Gb of size and need CPU times of more than 10 h for single geometry calculations on a single CPU. The consequence is that the calculations become unfeasible on the usual nodes of the grid which are heterogeneous and have fairly small memories. This means that for the application considered here it is either necessary to select the few parallel machines available on the grid or a device able to reroute related jobs to HPC platforms. Data reported in Table 2 show, in fact, that when increasing the number of processors, the CPU time for a single calculation speeds up considerably despite the fact that an increase of the overall allocated memory is necessary, due to the fact that GAMESS-US, when working in parallel, replicates parts of the memory on each

Table 2. CPU time and memory allocations for CCSD(T) calculations with four different basis sets of increasing dimension.

	CPU time [sec] CPU[a] number				Memory [MBytes] CPU[a] number			
Basis set	1	2	4	8	1	2	4	8
cc-pVDZ	11	16	9	7	36	44	59	90
cc-pVTZ	368	291	182	105	292	322	383	505
cc-pVQZ	7837	4394	2762	1698	1922	2181	2700	3737
cc-pV5Z	36610	24724	12744	8492	5540	6112	7256	9545

The results for various number of processors are shown. [a] Calculations performed on quad-core Nehalem EX (2.8 Ghz) cpus.

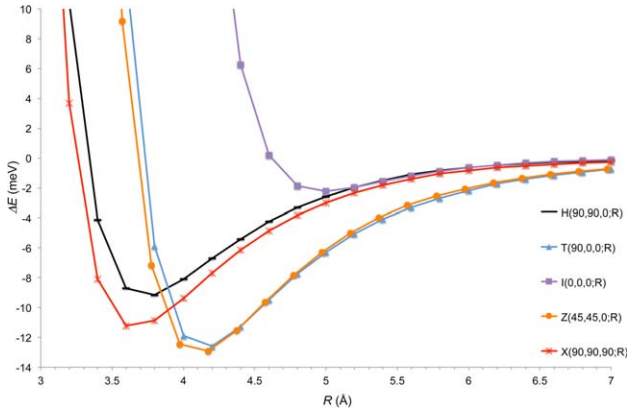

Figure 3. Long range CCSD(T)/cc-pV5Z potential energy curves ΔE plotted as a function of R for the X-shape, H-shape, T-shape, Z-shape, and I-shape arrangements. [Color figure can be viewed in the online issue, which is available at wileyonlinelibrary.com.]

computing element. This prompted the choice of using the GAMESS-US package offered as a grid service via SSH on the SP6 machine of CINECA[40] by the COMPCHEM VO. The use of SSH allowed the use of the parallel version of the electronic structure *ab initio* package GAMESS-US 2009, available on the CINECA HPC platform through a cross submission from the EGI grid, using gLite middleware. This allowed us to repeat at the CCSD(T) level of theory the extended *ab initio* calculations of the electronic structure for all the arrangements reported in Table 1. For illustrative purposes, the calculated intermolecular pair potential of N_2-N_2, ΔE, the difference between the energy of the dimer in the given geometry and the isolated monomer energies computed at the CCSD(T) level of theory, related to the H, X, T, I, and Z arrangements are shown in Figure 3 in which the improved long range interaction energy is plotted as a function of R in the range 3–7 Å. As apparent from the figure the H, X, T, and Z arrangement long range parts of the curves ($R \geq 3.4$ Å) is similar. They all show the forming, in fact, of van der Waals clusters having an energy minimum of more than 8.67 meV in the interval of R values located from just above 3.5 Å for the H and X-shape, to just below 4.2 Å for the T and X-shapes. Also, the long range part of the I curve shows a minimum associated with a van der Waals cluster though with a much smaller energy minimum, about 2.17 meV, located at much larger R values (about 5 Å). In order to get a more accurate estimate of the energy well depth, the five different curves have been interpolated in the region close to the minimum using a polynomial of the third order. The minimum energy and the associated intermolecular distance R values obtained from the interpolation are shown in Table 3

Table 3. Interpolated minimum energy and related position for the five investigated configurations.

	H	X	T	Z	I
R [Å]	3.74	3.64	4.15	4.11	4.98
ΔE [meV]	9.3782	11.552	12.833	13.186	2.2914

The intermolecular bonds are fixed at their experimental equilibrium distance (1.094 Å).

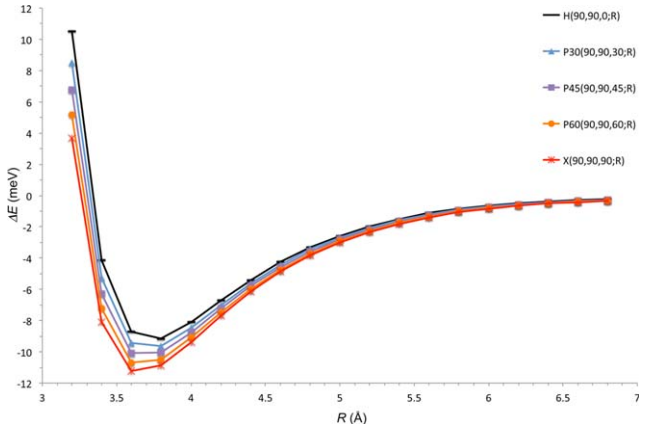

Figure 4. Long range CCSD(T)/cc-pV5Z potential energy curves ΔE plotted as a function of R at different values of Φ. [Color figure can be viewed in the online issue, which is available at wileyonlinelibrary.com.]

where the related ΔE values are also reported. An interesting feature of the results is that the T and Z arrangements lead to the most stable van der Waals geometries, whereas the X and H arrangements allow a close encounter of the two nitrogen molecules enhancing, so far, the likelihood of an N atoms exchange. Because of our interest on the reactive exchange path in the $N_2 + N_2$ collisional process, we spent additional computational effort to investigate the possibility of interconverting the parallel (H-shape) and the crossed (X-shape) arrangements which, after all, also in our previous calculations[14] led to the innermost repulsive barrier. The importance of these two arrangements is also confirmed by the presence of two bound states on the singlet $(^1\Sigma_g^+)$ PES[41] of the same symmetry of the parallel (D_{2h}) and crossed (D_{2d}) configurations. To confirm this, we performed some CASSCF(12,12) geometry optimizations with symmetry constraints. The calculations enabled us to identify two relative minima of symmetry D_{2h} and T_d (the D_{2d} is the largest Abelian subgroup of the T_d group). In Figure 4, the long range CCSD(T) potential energy values ΔE are plotted as function of R, for the H, X, P30, P45, and P60 arrangements. H and X arrangements show in the long range region well depth of 9.38 meV, with the minimum located at $R = 3.74$ Å, and 11.55 meV, with the minimum located at $R = 3.64$ Å, respectively. Moreover, in going from the H to the X arrangement the location on R of the minimum lowers gradually, whereas the depth increases. Moving to shorter range not truly stable molecular structures were singled out (see Fig. 5 in which the short range region is extended down to 1 Å). Figure 5 shows that when R decreases ΔE in general increases, though the possibility of a shifting from one channel to another is not excluded. As a matter of fact, the X, T, and I arrangements exhibit a local minimum that follows, as R decreases, a first maximum located at larger distances and moves to lower R values in going from I to X, suggesting possible interchanges between different arrangements especially when the constraint of setting r_a and r_b at the equilibrium value is released. For this reason, further investigations were carried out by calculating the evolution of ΔE of the H and X arrangements when one or both intramolecular distances are stretched with respect to the N_2 equilibrium distance. In particular, as shown in Table 1, the internuclear distances were varied by 0.4 to 0.6 Å (see Fig. 6 for the plot of ΔE of the H and X arrangements).

CCSD(T) Fit

Unfortunately, when one or both internuclear distances are stretched with respect to their equilibrium values the role of nondynamical correlation energy becomes important and the wavefunction of the system cannot be properly described by a single determinant. Nonetheless, in order to have a (higher level than before) *ab initio* description of the interaction for nonequilibrium internuclear distances of N_2, all the energy values calculated at the CCSD(T) level were considered for the purpose of fitting the PES using the Paniagua computational procedure gfit4c,[42] that is embodied into GEMS. An advantage of such procedure is that it is possible to correct the *ab initio* values found to be inappropriate either for the fitting or for dynamical calculations. Another advantage of the adopted procedure is the fact that it is based on the many body expansion (MBE) method of Sorbie and Murrell,[43] that builds an N-body potential by progressively adding contributions of the N-k (where k goes from 1 to N-1) type. This allows the reuse of the already established lower dimension terms, both for the values and for functional representation of the PES, and the enforcing on them of physically grounded constraints, like spectroscopic and dynamical information. The expression of the MBE for a four-atom system is given as a sum of 1-body (1), 2-body (2), 3-body (3), and 4-body (4) terms as follows:

$$\begin{aligned} V(r_a, r_b, \theta_a, \theta_b, \Phi, R) &= V_A^{(1)} + V_B^{(1)} + V_C^{(1)} + V_D^{(1)} \\ &+ V_{AB}^{(2)}(\xi_{AB}) + V_{AC}^{(2)}(\xi_{AC}) + V_{BC}^{(2)}(\xi_{BC}) \\ &+ V_{AD}^{(2)}(\xi_{AD}) + V_{BD}^{(2)}(\xi_{BD}) + V_{CD}^{(2)}(\xi_{CD}) \\ &+ V_{ABC}^{(3)}(\xi_{AB}, \xi_{BC}, \xi_{AC}) + V_{ABD}^{(3)}(\xi_{AB}, \xi_{BD}, \xi_{AD}) + V_{ACD}^{(3)}(\xi_{AC}, \xi_{AD}, \xi_{CD}) \\ &+ V_{BCD}^{(3)}(\xi_{BC}, \xi_{CD}, \xi_{BD}) + V_{ABCD}^{(4)}(\xi_{AB}, \xi_{AC}, \xi_{AD}, \xi_{BC}, \xi_{BD}, \xi_{CD}) \end{aligned} \quad (1)$$

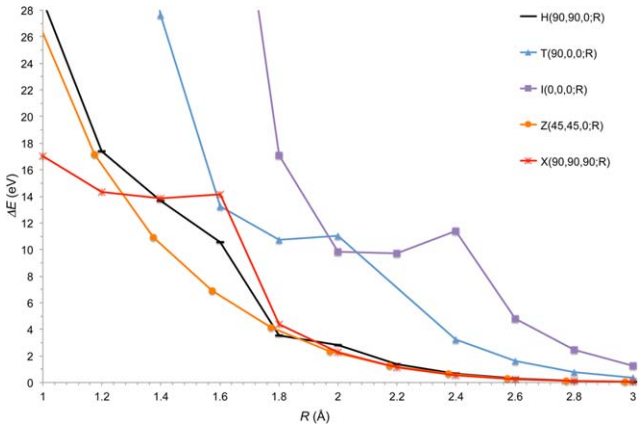

Figure 5. Short range CCSD(T)/cc-pV5Z potential energy values ΔE plotted as a function of R. [Color figure can be viewed in the online issue, which is available at wileyonlinelibrary.com.]

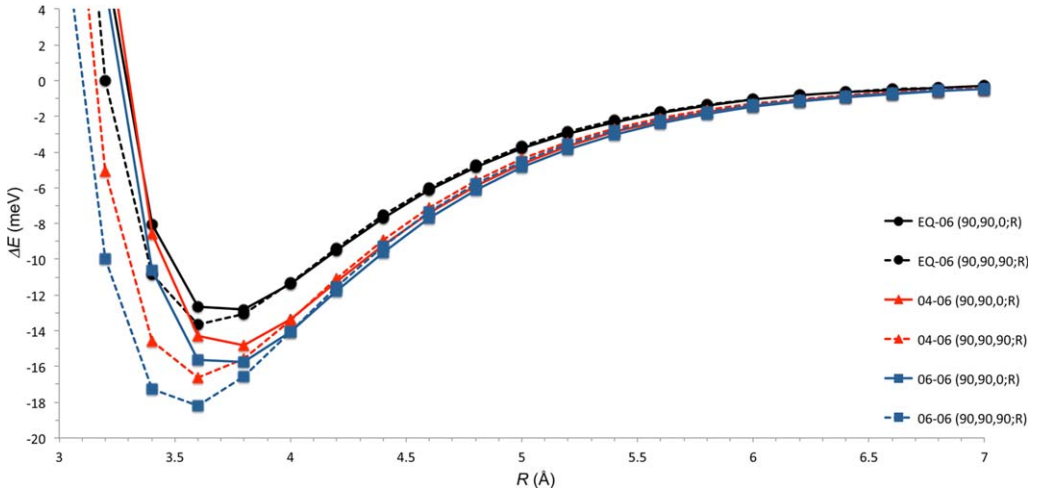

Figure 6. CCSD(T)/cc-pV5Z Van der Waals potential energy curves ΔE plotted as a function of R of the three stretched geometries for the H and X arrangements. The solid circle symbols [with either solid (90,90,0; R) or dashed (90,90,90; R) line] refer to the arrangements with one internuclear distance at the equilibrium and the other one stretched by 0.6 Å (EQ-06); the solid triangles [with either solid (90,90,0; R) or dashed (90,90,90; R) line] refer to the arrangements with one distance stretched by 0.4 Å and the other one by 0.6 Å (04-06), whereas the solid squares [either solid (90,90,0; R) or dashed (90,90,90; R) line] refer to the arrangements with both internuclear distances stretched by 0.6 Å (06-06). [Color figure can be viewed in the online issue, which is available at wileyonlinelibrary.com.]

in which for sake of simplicity the four N atoms are called A, B, C, D, and ξ is an appropriate function of the relative positions of the nuclei. The 1-body terms $V^{(1)}$ are the electronic energies of the atoms in the appropriate dissociation configuration. For the N_2 + N_2 electronic ground state PES these terms were set equal to zero. In the Paniagua approach embodied in the gfit4c routines adopted by us, ξ is defined as a function of the internuclear distances r_{ij} and the 2-body components (say $V^{(2)}_{AB}(\xi_{AB})$) of the potential are expressed as:

$$V^{(2)}_{AB}(\xi_{AB}) = \frac{c_{0AB}e^{-\alpha_{AB}r_{AB}}}{r_{AB}} + \sum_{s=1}^{S} c_{sAB}\rho^{s}_{AB} \quad (2)$$

in which ρ_{AB} is a Rydberg-like variable formulated as:

$$\rho_{AB} = r_{AB}e^{-\beta^{(p)}_{AB}r_{AB}}, p = 2, 3, \text{or } 4 \quad (3)$$

with p being chosen as in Ref. [44]. The c_{sAB} coefficients, including $s = 0$, as well as the non linear parameters $\beta^{(p)}_{AB}$ were evaluated by fitting the 2-body *ab initio* values and S is the chosen order of the polynomial. The 3-body terms (say $V^{(3)}_{ABC}(\xi_{AB}, \xi_{AC}, \xi_{BC})$) were expressed in terms of polynomials of order N in the same Rydberg-like variables ρ_{AB}, ρ_{AC}, and ρ_{BC}:

$$V^{(3)}_{ABC}(\xi_{AB}, \xi_{AC}, \xi_{BC}) = \sum_{lmn}^{N} d_{lmn}\rho^{l}_{AB}\rho^{m}_{AC}\rho^{n}_{BC} \quad (4)$$

with the d_{lmn} coefficients being evaluated by fitting the 3-body ABC *ab initio* values. Finally, also the functional form chosen to express the 4-body term $V^{(4)}_{(ABCD)}(\xi_{AB}, \xi_{AC}, \xi_{AD}, \xi_{BC}, \xi_{BD}, \xi_{CD})$ was written, similarly to what has been done for the 3-body term, in terms of a polynomial of order N in the Rydberg-like variables ρ_{AB}, ρ_{AC}, ρ_{AD}, ρ_{BC}, ρ_{BD}, and ρ_{CD}:

$$V^{(4)}_{ABCD} = \sum_{ijklmn}^{N} e_{ijklmn}\rho^{i}_{AB}\rho^{j}_{AC}\rho^{k}_{AD}\rho^{l}_{BC}\rho^{m}_{BD}\rho^{n}_{CD} \quad (5)$$

where appropriate constraints are imposed on the indices in order to guarantee the right behavior of the polynomial in all regions of the configuration space.

In order to carry out the fitting of the N_2-N_2 PES, we used the following sets of *ab initio* points: 1440 2-body values, 4320 3-body values, and 1917 4-body values. Moreover, both experimental and *ab initio* information taken from previous work on the $N + N_2(^1\Sigma^+_g)$ PES[45,46] were used to tune both the 2- and 3-body terms.

The zero of all the *ab initio* electronic energy values was set at the minimum of the dissociation energy of $(N_2)_2$ into $2N_2$. The scaling value has been calculated at the CCSD(T) level of theory using the cc-pV5Z basis set. In particular, we calibrated the calculated potential energy values with respect to the energy point obtained by increasing R to a large distance (20 Å) and by matching the obtained value with the one associated with the isolated nitrogen molecules (−218.82612523 Hartree).

The fitted 2- and 3-body components of the potential, both fitted to a polynomial of order 6, show a root mean square deviation of 0.005 and 0.05 eV, respectively. The root mean square deviation of the 4-body term is 0.2 eV, with the largest deviation of 2 eV occurring in the highly repulsive region. The fitted PES provides a dissociation energy of 9.82 eV at an equilibrium distance of 1.099 Å, in good agreement with the experimental values (1.094 Å and 9.52 eV,[47,48] respectively).

To investigate the main features of the fitted PES, several fixed arrangement isoenergetic contour plots were drawn as a function of the relevant distances. A typical plot of this type is the one given in Figure 7, in which the isoenergetic contours for the H arrangement are plotted as a function of R and

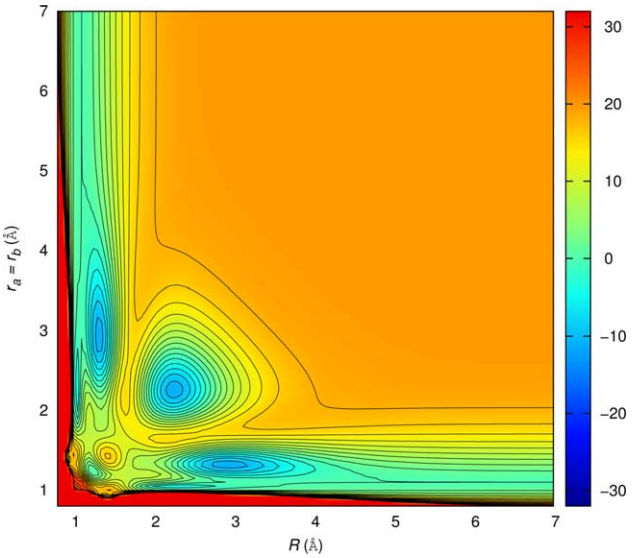

Figure 7. CCSD(T)/cc-pV5Z isoenergetic contour plots for the H arrangement with $r_a = r_b$. Energy contours are drawn every 2 eV.

$r_a = r_b$. The H contour plots show that while the N_2 molecules approach each other the minimum energy path (MEP) of the PES shifts to $r_a = r_b$ values larger than equilibrium and deepens by ending up to stabilize (−27.71 eV) a rectangular geometry of size R =3 Å and $r_a = r_b \simeq 1.3$ Å. Such entrance channel structure is mirrored in a corresponding product channel one in which the two N_2 molecules have interchanged symmetrically one N atom (R is now about 1.3 Å, whereas r_a and r_b increase equally all along the channel). The reactant and product channels communicate mainly via a double barrier structure of about 15 eV, separated by a deep well (−26.04 eV) centered on $R = 2.2$ Å and $r_a = r_b$ about 2.5 Å. The two channels communicate also via a narrower channel exhibiting a lower double barrier structure at shorter distances. These are indeed likely exchange reactive paths going through the N_4 square minimum and associated with the insertion with two differently stretched N_2 geometries before flying away on the other side. However, it cannot be excluded that the energetics of such MEP_s is strongly affected by the $r_a = r_b$ constraint on the H geometry. As a matter of fact, this effect weakens for the X arrangement contour plots (see related plots of Fig. 8). The X contour plots show, in fact, that while the entrance channel well associated with a distorted rectangular (or tetrahedral like) structure is located at approximately the same R and $r_a = r_b$ values, the well associated with the shorter R N_4 structure is much deeper (−60 eV) and is located at $R \simeq 1.8$ Å and $r_a = r_b \simeq 2.4$ Å. The related MEP, though still competing with a shorter R lower barrier reactive channel, has an energetically favoured geometry interchange dynamics in the region sandwiched by the two symmetric, on the opposite side of the crossed N_2 molecule, 7.7 eV barriers located at $R \simeq 3$ Å and $r_a = r_b = 1.6$ Å.

Higher Level Calculations

A first higher level correction to our CCSD(T) calculated values is the adoption of the aug-cc-pV5Z basis set as proposed in Ref. [25]. However, as expected,[49] the values reported in Ref. [25] for the H and X arrangements differ only by a few thousandths of eV from our CCSD(T) ones. Therefore, in order to replace our CCSD(T) values computed at N_2 internuclear distances differing from the equilibrium value (as already mentioned the N_4 wavefunction is not properly described by a single determinant due to the role played by nondynamical correlation) and used for the fitted PES described in the previous section, we carried out MR calculations. This is expected to be particularly important in our case because of our interest into the investigation of the N atom exchange channels which involve the short range region of the PES where the two molecules get very close and configurations having one or both stretched interatomic distances, including bond breaking and forming, become important. To this end, the MRPT2 procedure implemented in GAMESS-US[50,51] was adopted using, as before, the cc-pV5Z basis set. More in detail, it was chosen to correlate the two degenerate π_{2p} orbitals and the σ_{2p} orbital of each molecule while the inner σ orbitals were kept frozen at the SCF level. Using this level of theory, we repeated the calculation for the H, X, P15, P30, P45, P60, and P75 arrangements which are believed to be very important for the description of reactive channels. For the just mentioned arrangements, the internuclear distance pairs investigated are the following:

- $r_a = r_b = 1.094$ Å and R varying from 1 to 5 Å
- $r_a = 1.094$, $r_b = 1.694$ Å and R varying from 1 to 5 Å
- $r_a = 1.494$, $r_b = 1.694$ Å and R varying from 1 to 5 Å
- $r_a = 1.694$, $r_b = 1.694$ Å and R varying from 1 to 5 Å

Moreover, also some other calculations were performed at larger and shorter values of R. The results of the MRPT2 calculations are shown in Figures 9–12. As in the case of the CCSD(T) calculations, the potential energy zero is set at the complete dissociation of the two monomers.

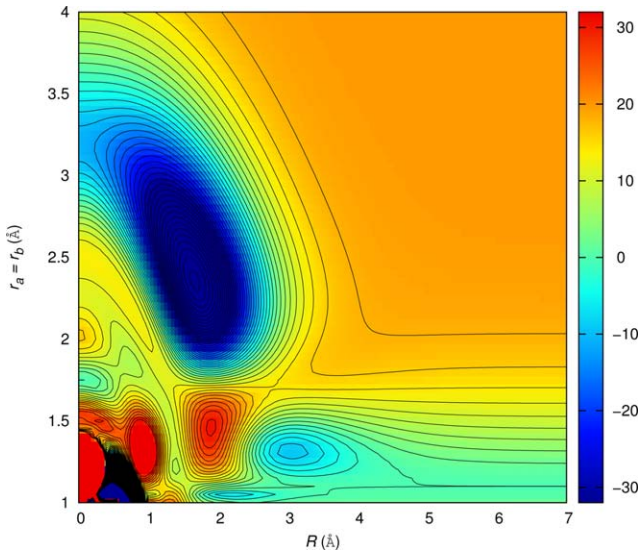

Figure 8. CCSD(T)/cc-pV5Z isoenergetic contour plots for the X arrangement with $r_a = r_b$. Energy contours are drawn every 2 eV.

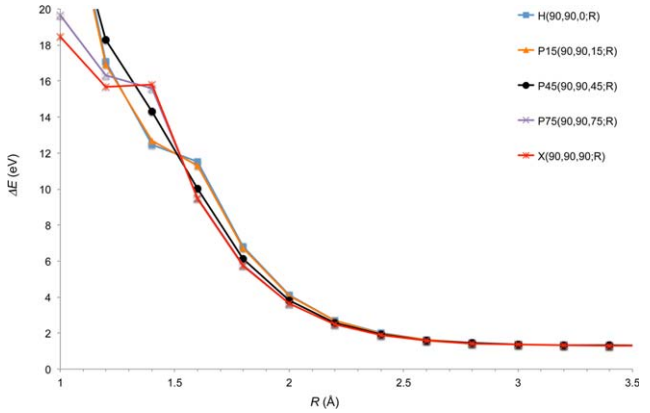

Figure 9. Short range MRPT2/cc-pV5Z potential energy values plotted as a function of R for different values ΔE of Φ. The interatomic distances of each N_2 molecule are kept fixed at the equilibrium value (r_a=r_b=1.094 Å). [Color figure can be viewed in the online issue, which is available at wileyonlinelibrary.com.]

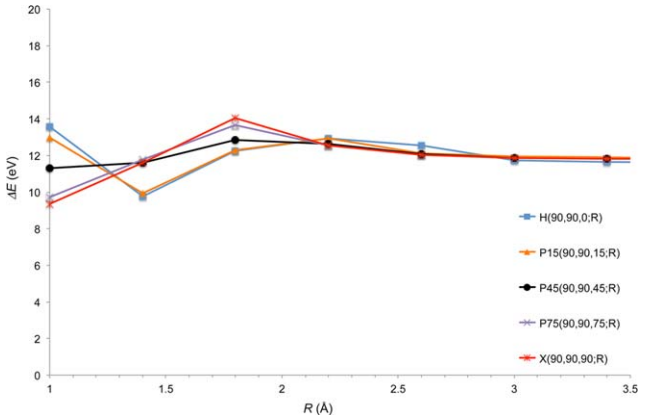

Figure 11. Short range MRPT2/cc-pV5Z potential energy values plotted as a function of R for different values ΔE of Φ. One interatomic distance is stretched by 0.6 Å and the other one by 0.4 Å (r_a=1.494 Å, r_b=1.694 Å). [Color figure can be viewed in the online issue, which is available at wileyonlinelibrary.com.]

When the internuclear distances are at their equilibrium values the MRPT2 results confirm the CCSD(T) ones. This is apparent from a comparison of the ΔE plot for the H and X arrangements given in Figure 9 with the corresponding results of Figure 5 (mean square deviation = 4.3%). Moreover, the positions and heights of the energy barriers singled out by the two methods are also in satisfactory agreement, further confirming the good quality of the CCSD(T) calculations for these arrangements. The real difference is the value of the asymptotic limit due to the different methods used for calculating the energy zero (the CCSD(T) method leads to a partial recovery of the dynamical correlation larger than that given by the MRPT2 one). This difference was estimated to be 1.3 eV, for the H arrangements, and was used to match MRPT2 and CCSD(T) results for the fitting.

MR corrections provide interesting indications on the mechanisms of bond breaking and forming. In Figure 10, the H and X short range potential energy values calculated with r_a = 1.094 Å and r_b = 1.694 Å show that at R = 3 Å (right-hand side of the figure) the potential energy values are larger, with respect to the asymptote, if compared to the values for the non stretched arrangement given in Figure 5. This confirms the fact that R = 3 Å is already sufficiently "asymptotic" to make the potential energy of the molecular geometries with stretched N_2 molecules larger than that of the geometries with the N_2 molecules at equilibrium. On the contrary, in the region of R ranging from 1 to 2 Å the potential energy values associated with the geometries with N_2 molecules having internuclear distances shorter than the equilibrium value are lower than those of the non stretched arrangement and this results in a lower barrier to N exchange. In particular, for the X arrangement, this difference is really large (at R = 1 Å it is about 7 eV) implying the likelihood of an arrangement change. If both N_2 internuclear distances are stretched such effect becomes more evident. In Figures 11 and 12, the N_2 asymmetric (r_a = 1.494 Å, r_b = 1.694 Å) and the N_2 symmetric (r_a = r_b = 1.694 Å) stretching potential energy values are plotted. Both the figures confirm, in the short range region

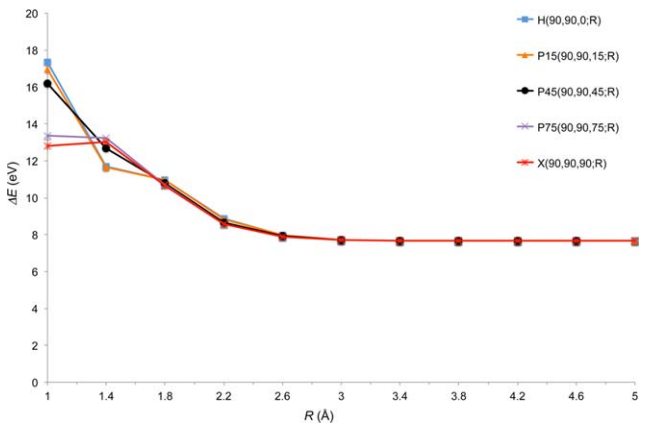

Figure 10. Short range MRPT2/cc-pV5Z potential energy values plotted as a function of R for different values ΔE of Φ. One interatomic distance is stretched by 0.6 Å and the other is kept fixed at its equilibrium value (r_a=1.094 Å, r_b=1.694 Å). [Color figure can be viewed in the online issue, which is available at wileyonlinelibrary.com.]

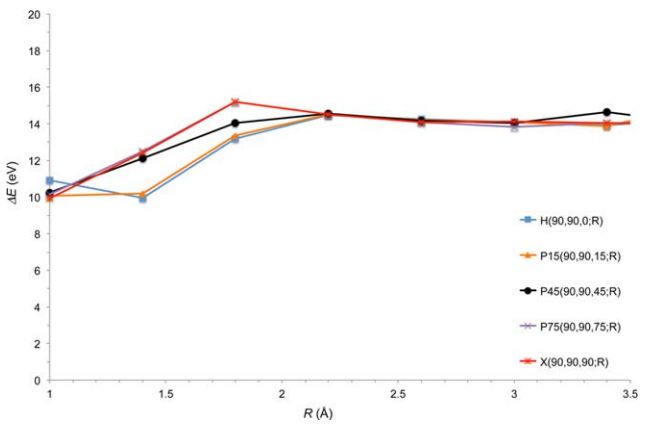

Figure 12. Short range MRPT2/cc-pV5Z potential energy values plotted as a function of R for different values ΔE of Φ. Both interatomic distances are stretched by 0.6 Å (r_a=1.694 Å, r_b=1.694 Å). [Color figure can be viewed in the online issue, which is available at wileyonlinelibrary.com.]

($1 < R < 2$), the possibility for a reactive channel opening associated with the change in the arrangement of $(N_2)_2$.

As a result for the new fitting, we used the denser matrix of the CCSD(T) results for arrangements characterized by both N_2 at the equilibrium distance and the coarser matched MRPT2 ones for arrangements having one or both N_2 internuclear distances stretched from the equilibrium value.

MRPT2 PES

The MRPT2 potential energy values were fitted using again the Paniagua et al. procedure.[42] The data set is made by a collection of both scaled MRPT2 and CCSD(T) energy values. Altogether, we have assembled within the GEMS scheme 1440 2-body points, fitted to a polynomial of order 6, 4320 3-body values, fitted to a polynomial of order 6, and 1361 4-body values, fitted to a polynomial of order 8. For this new fitting, we obtained an average standard deviation of 0.27 eV and a maximum error of 1.52 eV, located in the inaccessible strongly repulsive region. A comparison of the MRPT2 PES with the CCSD(T) one has been performed graphically in Figures 13 and 14 by drawing the same contour plots as in Figures 7 and 8. As a matter of fact, the MRPT2 isoenergetic contours for the H arrangements are plotted in Figure 13 as a function of R and $r_a = r_b$. The plot exhibits significant differences with respect to the CCSD(T) contours plot given in Figure 7. The most apparent feature of the MRPT2 contour plots is the disappearance of the deep well associated with the square N_4 structure and the consequent weakening of competition between the large and the small R values transition state MEP_S. Obviously, this does not unequivocally exclude the possibility that such a structure can arise for different cross sections of the PES. Yet, it singles out a smoother, less internal energy mode coupling N atom exchange process. The same type of smoothing is shown by the contour plots of the X

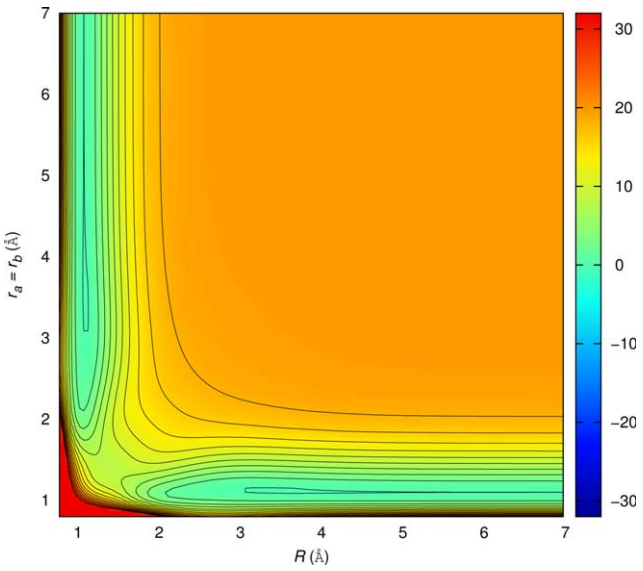

Figure 13. MRPT2/cc-pV5Z isoenergetic contour plots for the H arrangement with $r_a = r_b$. Energy contours are drawn every 2 eV. [Color figure can be viewed in the online issue, which is available at wileyonlinelibrary.com.]

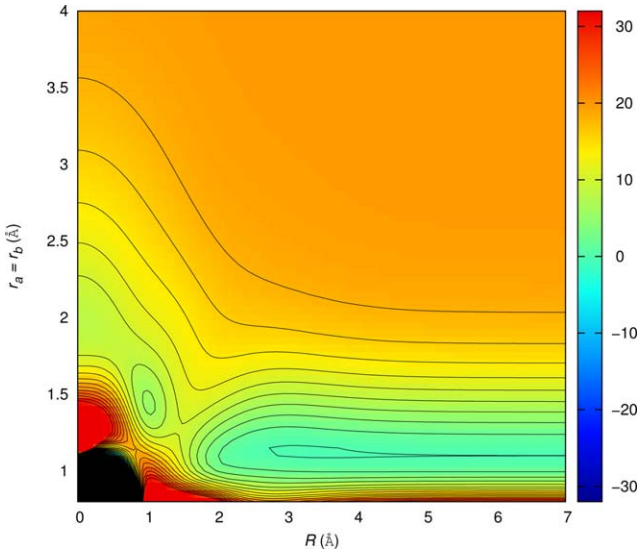

Figure 14. MRPT2/cc-pV5Z isoenergetic contour plots for the X arrangement with $r_a = r_b$. Energy contours are drawn every 2 eV. [Color figure can be viewed in the online issue, which is available at wileyonlinelibrary.com.]

arrangement (see Fig. 14) in which the large R well disappears to give way (amplified) to a short R MEP. In Figure 14, the short R double well structure has a smoother shape than that of Figure 8. Also in this case, therefore, the conclusion is that the energy interchange between the different internal modes can lead to reactive N atom exchange.

Conclusions

The assemblage of a GEMS, meant to operate as a computational engine of multiscale complex simulations for technological innovations, has allowed us to start a process in which the efficiency of the $N_2 + N_2$ collision processes in capturing or releasing internal energy will be quantitatively estimated using dynamical treatments. In this article, the first step of such processes is described: the *ab initio* determination of the PES for which we had to (a) combine different high level electronic structure calculations and (b) bridge HTC computing with HPC. These two elements have allowed us, via a progression from CCSD(T) to MR calculations and the scaling and matching of the obtained results, to assemble a set of data suitable for a full range description of the reactive and nonreactive interaction. The PES obtained by fitting, using the procedure of Paniagua et al., such set of data shows interesting features of the competition between nonreactive and reactive paths to energy exchange in $N_2 + N_2$ collisions. The first added value of the present article is, therefore, the high level of *ab initio* quality of the simultaneous exploration of both reactive and nonreactive channels of the process. The second added value is the fact that, in the spirit of GEMS, the first step will be followed by a second step in which the fitted PES is tested using dynamical calculations and a comparison with experimental data. In GEMS, these steps are embodied within an iterative process in which extending and improving the calculation of the electronic structure, the fitting of the potential energy

values, the dynamical validation of the fitted PES and the statistical averaging of the detailed probabilities to work out virtual experimental values will constitute an invaluable cooperative optimization procedure and will allow the assemblage of a solid data base of rate coefficients for nitrogen involving processes.

The third added value of the article is the opportunity offered for implementing a working version of GEMS for four atom systems, previously confined to atom-diatom systems, and the related set of grid tools. In particular, this work has prompted the development of some tools selecting the most appropriate machine to work on (and in particular to bridge HTC and HPC machines) for heavy systems like the $N_2 + N_2$ one.

Acknowledgment

The authors wish to acknowledge CINECA (IT) for computing time on its platform and the COMPCHEM virtual organization.

Keywords: potential energy surface · electronic structure calculation · fitting · dynamics · *ab initio methods*

How to cite this article: L. Pacifici, M. Verdicchio, N. Faginas Lago, A. Lombardi, A. Costantini, *J. Comput. Chem.* **2013**, *34*, 2668–2676. DOI: 10.1002/jcc.23415

[1] M. Capitelli, Non-Equilibrium Vibrational Kinetics; Springer-Verlag: Berlin, **1986**.
[2] I. Armenise, M. Capitelli, E. Garcia, C. Gorse, A. Laganà, S. Longo, *Chem. Phys. Lett.* **1992**, *200*, 597.
[3] D. C. Knauth, B. G. Andersson, S. R. McCandliss, H. W. Moos, *Nature* **2004**, *429*, 636.
[4] D. J. Nesbitt, *Chem. Rev.* **1988**, *88*, 843.
[5] D. J. Nesbitt, A. van der Avoird, *J. Chem. Phys.* **2011**, *134*, 044314.
[6] M. Albertí, N. F. Lago, F. Pirani, *Chem. Phys.* **2012**, *339*, 232.
[7] R. J. Hinde, *J. Chem. Phys.* **2008**, *128*, 154308.
[8] A. Boothroyd, P. Martin, W. Keogh, M. Peterson, *J. Chem. Phys.* **2002**, *116*, 666.
[9] A. Ceballos, E. Garcia, A. Rodriguez, A. Laganà, *J. Phys. Chem. A* **2001**, *105*, 1797.
[10] A. Ceballos, E. Garcia, A. Rodriguez, A. Laganà, *Chem. Phys. Lett.* **1999**, *305*, 276.
[11] A. Ceballos, E. Garcia, A. Rodriguez, A. Laganà, *J. Phys. Chem. Ref. Data* **2002**, *31*, 371.
[12] A. Ceballos, E. Garcia, A. Laganà, *Phys. Chem. Chem. Phys.* **2002**, *4*, 5007.
[13] E. Garcia, A. Saracibar, A. Sanchez, C. Laganà, *J. Phys. Chem. A* **2009**, *113*, 14312.
[14] M. Verdicchio, L. Pacifici, A. Laganà, *Lect. Notes Comput. Sci.* **2012**, *7333*, 371.
[15] A. Laganà, F. Pirani, E. Garcia, M. Bartolomei, M. Cacciatore, M. Rutigliano, Submitted for publication.
[16] J. C. Raich, N. S. Gillis, *J. Chem. Phys.* **1977**, *66*, 846.
[17] T. B. MacRury, W. A. Steele, B. J. Berne, *J. Chem. Phys.* **1976**, *64*, 1288.
[18] P. S. Y. Cheung, J. G. Powles, *Mol. Phys.* **1976**, *32*, 1383.
[19] V. Aquilanti, M. Bartolomei, D. Cappelletti, E. Caramona-Novillo, F. Pirani, *J. Chem. Phys.* **1998**, *93*, 485.
[20] L. Gomez, B. Bussery-Honvault, T. Cauchy, M. Bartolomei, D. Cappelletti, F. Pirani, *Chem. Phys. Lett.* **2007**, *445*, 99.
[21] A. van der Avoid, P. E. S. Wormer, A. P. J. Jansen, *J. Chem. Phys.* **1986**, *84*, 1629.
[22] D. Cappelletti, F. Vecchiocattivi, F. Pirani, F. R. W. McCourt, *Chem. Phys. Lett.* **1996**, *248*, 237.
[23] S. W. M. Huo, S. Green, *J. Chem. Phys.* **1996**, *104*, 7572.
[24] J. R. Stallcop, H. Partridge, *Chem. Phys. Lett.* **1997**, *281*, 212.
[25] R. Hellmann, *Mol. Phys.* **2013**, *111*, 387.
[26] A. Laganà, N. Balucani, S. Crocchianti, P. Casavecchia, E. Garcia, A. Saracibar, *Lect. Notes Comput. Sci.* **2011**, *6784*, 453.
[27] A. Laganà, E. Garcia, A. Paladini, P. Casavecchia, N. Balucani, *Faraday Discuss.* **2012**, *157*, 415.
[28] A. Laganà; in "Theory of chemical reaction dynamics", A. Laganà and G. Lendvay A. Eds.; Kluver Academic Publishers, Dordrecht Boston London, **2004** 145, 363–380.
[29] A. Costantini, O. Gervasi, C. Manuali, N. Faginas Lago, S. Rampino, A. Laganà, *J. Grid Comput.* **2010**, *8*, 571.
[30] S. Rampino, A. Monari, E. Rossi, S. Evangelisti, A. Laganà, *Chem. Phys.* **2012**, *398*, 192.
[31] The European Grid Infrastructure, Available at www.egi.eu, accessed on January 13, 2013.
[32] A. Laganà, A. Riganelli, O. Gervasi, *Lect. Notes Comput. Sci.* **2006**, *3980*, 665.
[33] C. Møller, M. S. Plesset, *Phys. Rev.* **1934**, *46*, 618.
[34] S. F. Boys, F. Bernardi, *Mol. Phys.* **1970**, *19*, 553.
[35] P. J. Hay, R. T. Pack, R. L. Martin, *J. Chem. Phys.* **1984**, *81*, 1360.
[36] M. W. Schmidt, K. K. Baldridge, J. A. Boatz, S. T. Elbert, M. S. Gordon, J. J. Jensen, S. Koseki, N. Matsunaga, K. A. Nguyen, S. Su, T. L. Windus, M. Dupuis, A. Montgomery, *J. Comput. Chem.* **1993**, *14*, 1347.
[37] M. S. Gordon, M. W. Schmidt, in "Theory and Applications of Computational Chemistry: the first forty years"C. E. Dykstra, G. Frenking, K. S. Kim, G. E. Scuseria (editors), Elsevier, Amsterdam, **2005**. pp. 1167–1189
[38] D. Feller, *J. Chem. Phys.* **1996**, *17*, 1571.
[39] K. Schuchardt, B. Didier, T. Elsethagen, L. Sun, V. Gurumoorthi, J. Chase, J. Li, T. Windus, *J. Chem Inf. Model.* **2007**, *47*, 1045.
[40] CINECA (IT), Available at www.cineca.it, accessed on April 21, 2013.
[41] T. J. Lee, J. E. Rice, *J. Chem. Phys.* **1991**, *94*, 1215.
[42] A. Aguado, C. Tablero, M. Paniagua, *Comput. Phys. Commun.* **2001**, *134*, 97.
[43] K. S. Sorbie, J. N. Murrell, *Mol. Phys.* **1975**, *52*, 1387.
[44] A. Aguado, C. Suarez, M. Paniagua, *J. Chem. Phys.* **1994**, *101*, 404.
[45] E. Garcia, A. Saracibar, S. Gomez-Carrasco, A. Laganà, *Phys. Chem. Chem. Phys.* **2008**, *10*, 2552.
[46] P. J. S. B. Caridade, B. R. L. Galvao, A. J. C. Varandas, *J. Phys. Chem. A* **2010**, *114*, 6063.
[47] E. J. Baerends, D. E. Ellis, P. Ros, *Chem. Phys.* **1973**, *2*, 41.
[48] T. Ziegler, J. G. Snijders, E. J. Baerends, *J. Chem. Phys.* **1981**, *74*, 1271.
[49] K. Patkowski, *J. Chem. Phys.* **2013**, *138*, 154101.
[50] K. Hirao, *Chem. Phys. Lett.* **1992**, *190*, 374.
[51] K. Hirao, *Int. J. Quantum Chem.* **1992**, *S26*, 517.

Received: 25 June 2013
Revised: 26 July 2013
Accepted: 27 July 2013
Published online on 26 August 2013